J. Phys. IV France **10** (2000)
© EDP Sciences, Les Ulis

Electrical conductivity measurement in dense metal plasmas: Comparisons of several metals

A.W. DeSilva and J.D. Katsouros

Institute for Plasma Research, University of Maryland, College Park, Maryland 20742, U.S.A.

Abstract. We measure the electrical conductivity of strongly coupled metal plasmas in the temperature range 8-30 kK, in a density range from about 1/2 solid density down to about 10^{-3} times solid density. Plasma density is deduced from streak photography, and temperature deduced from energy input, using the LANL SESAME database. The results are compared with theoretical predictions of several authors. When conductivity is plotted vs. atom density, very little difference is seen between aluminum, iron, nickel, copper and tungsten plasmas.

1. INTRODUCTION

We have previously reported measurements of the electrical conductivity of copper and aluminum plasmas created by rapid vaporization of wire by an electrical current [1,2]. The metal states produced in this manner range in conditions from a high pressure liquid to plasmas having temperatures of 5,000 to 30,000K, and densities ranging from almost solid density down to about 10^{-3} times solid density. In this paper we compare the results of measurements of conductivities for aluminum, iron, nickel, copper, and tungsten.

2. METHOD

A wire (purity 99.9+%) of the metal under study, typically 0.125 - 0.250 mm in diameter and 26 mm long, is stretched between two electrodes immersed in a water bath . A capacitor bank is connected via a low inductance path to one of the electrodes. A rogowski belt surrounds the main electrode to measure the time derivative of the current, and a resistive voltage divider is used to measure voltage at the load. The growth of the plasma column diameter may be recorded by a streak camera. We assume that the plasma fills the column diameter uniformly, from which we deduce the plasma density. The electrical energy input to the wire before vaporization is taken from I^2R power, with R taken from published literature for solid and liquid metals. After vaporization begins, energy input is taken from measured VIdt, where the measured voltage has been corrected for reactive contributions. We infer the plasma temperature from the energy input to the wire, making use of the SESAME equation of state tables generated at the Los Alamos National Laboratory [3].

The plasma expansion drives a shockwave in the surrounding water, and the high pressure in the water behind the shock serves to inhibit the plasma column expansion. In order to determine the boundary conditions at the outer plasma radius, we must have a model for the propagation of the pressure pulse and resulting shockwave through the water. The response of the water is adequately described with a one-dimensional cylindrical Lagrangian code due to Plooster [4] using the equation of state for water given by Rice and Walsh [5]. An estimate of thermal energy transfer between plasma and water indicates that the thickness of the plasma-water transition layer grows to only a few microns on the timescale of the experiment, so the assumption of a sharp boundary between plasma and water seems justified. Making use of this code, along with the measured energy input and the SESAME data, we can compute all necessary parameters of the plasma development in time. Comparison of the plasma expansion as calculated numerically with the plasma diameter measured from the streak photo shows close agreement, lending confidence to our use of the numerical model to find the temperature.

Figure 1 displays the time record of a typical discharge. A single shot yields a record of the conductivity over a wide range of density, and at varying temperatures. From a large number of shots taken with varied conditions (bank charge voltage, added series impedance, wire diameter), we select results for selected temperatures.

Article published online by EDP Sciences and available at http://dx.doi.org/10.1051/jp4:2000535

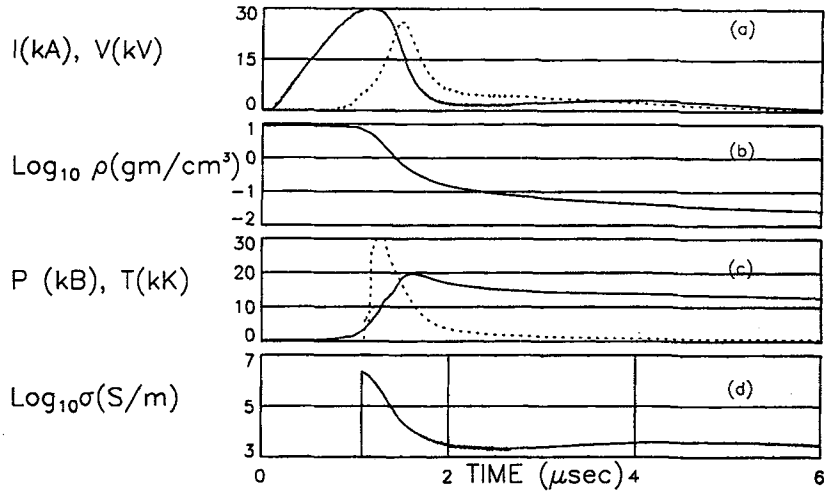

Figure 1. Time record of a discharge into a copper wire 0.25 mm in diameter, showing a) current (solid line), and voltage (dotted line), b) density, c) temperature (solid line) and pressure (dotted line), and d) conductivity as function of time. Energy input is calculated from voltage and current, and the rest of the curves are deduced from these data through use of the SESAME tables and the water compression model.

3. DATA ANALYSIS

In order to make clear the conditions through which the vapor/plasma passes, we display in Fig. 2 the isotherms of the pressure-volume relation from the SESAME database for aluminum, iron, and nickel, on which we have superposed the trajectory of typical single shots. Owing to the inertia of the water, the vapor may not expand freely, and the pressure rises rapidly after the temperature reaches the vaporization temperature, passes near the critical point, followed by further expansion with more or less additional heating, depending on the external parameters.

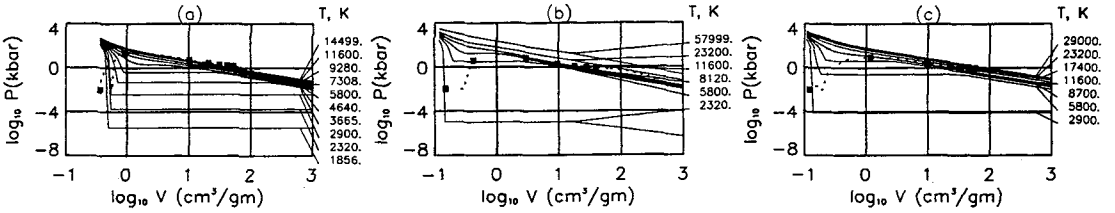

Figure 2. Isotherms of a) aluminum, b) nickel and c) iron from SESAME database, with superposed trajectories of the path followed by plasma conditions in typical shots. The square markers indicate 0.5 microsecond intervals.

We have noticed that in cases where current goes to zero, and subsequently restarts, the conductivity deduced from the time after the restrike may be much larger than that deduced from shots in which similar conditions of temperature and density were reached without the dip in current. We surmise that in the restrike, the current fails to flow uniformly, leading to a false conclusion. We therefore reject data from times following a drop in current to near zero.

Analysis of a large number of discharges, with varying charge voltages and external resistances allows us to find the conductivity at a variety of temperatures and densities. From individual shot profiles we select data at computed temperatures that lie within a narrow range (±3%) around a selected temperature, and plot the conductivity for these 'target' temperatures versus density. Results are shown in figures 3-7 for, respectively, aluminum, iron, nickel, copper, and tungsten.

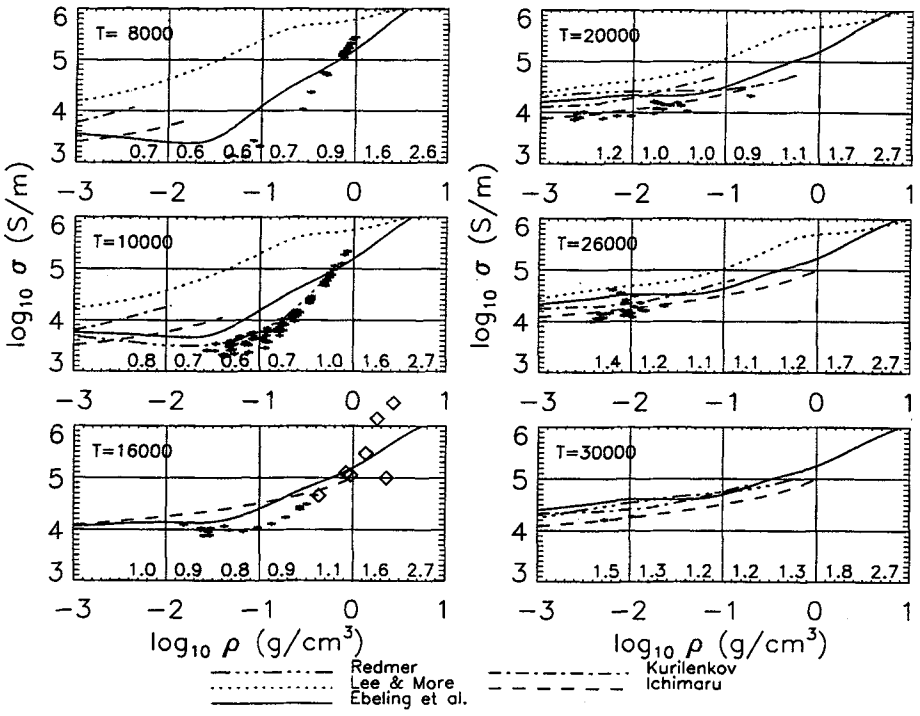

Figure 3: Electrical conductivity versus mass density for aluminum plasmas. Error bars on data indicate uncertainties due to digitization errors and to uncertainty in reading plasma column diameter from the streak photos. Numbers above the density axis indicate the effective ionization state from a Thomas-Fermi model by More [6]. Diamonds on 16kK plot are from theory of Dharma-wardana and Perrot [12].

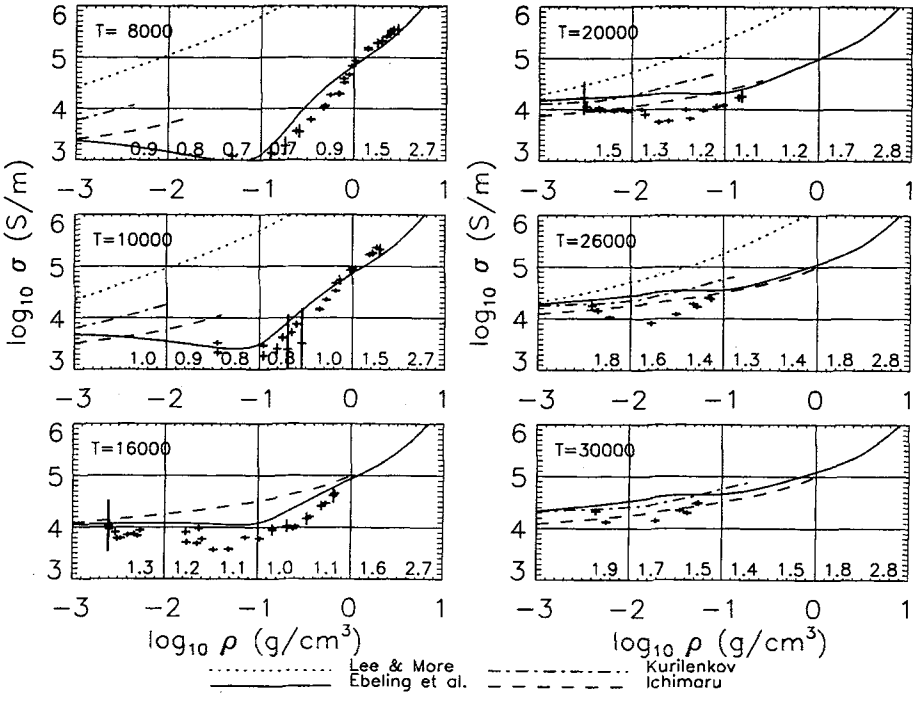

Figure 4. As in Fig. 3, for iron plasmas.

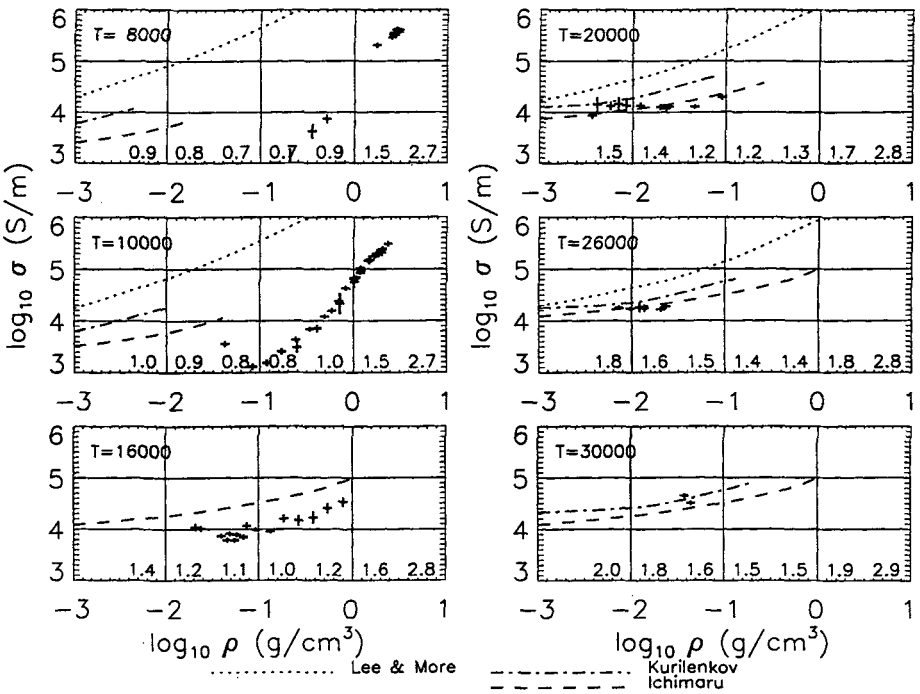

Figure 5. As in Fig. 3, for nickel plasmas.

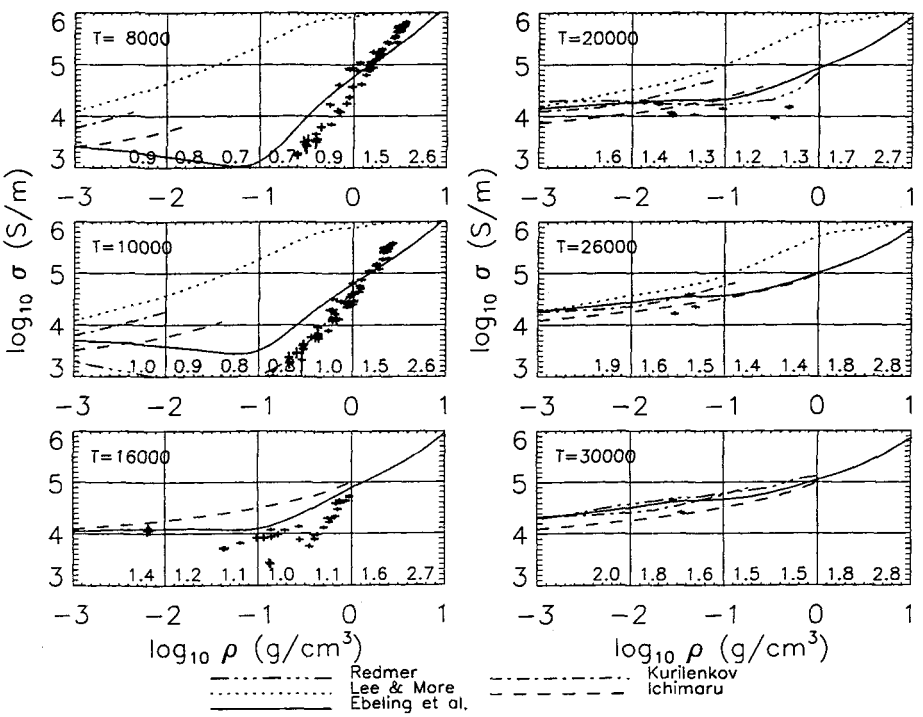

Figure 6. As in Fig. 3, for copper plasmas.

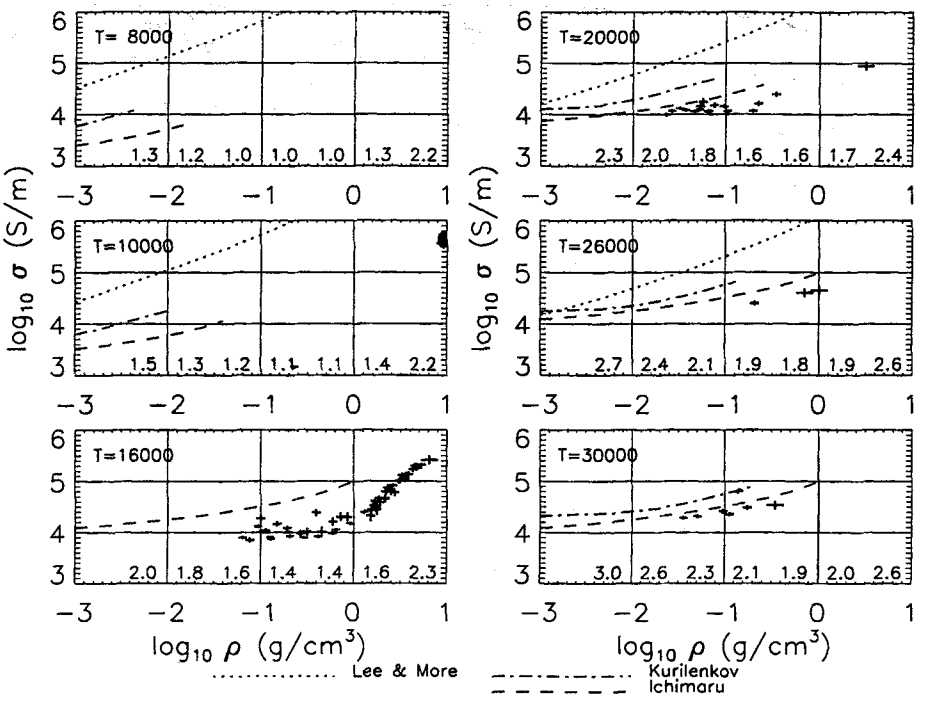

Figure 7. As in Fig. 3, for tungsten plasmas.

4. DISCUSSION

According to these measurements, the plasma conductivity is a strong function of the density, and at high density is almost independent of temperature. As the density falls, the effect of temperature is more apparent. For the lower temperatures we see that the conductivity falls to a minimum at a few percent of solid density, and then levels out or rises with further decrease in density, eventually approaching the Spitzer conductivity [7] that is valid for tenuous plasmas.

Theoretical models for the conductivity of strongly coupled plasmas versus mass density have been given by a number of authors. We have shown in Figs. 3-7 the results, where available, of theories of Redmer [8], Ebeling et al.[9], Ichimaru and Tanaka [10], Kurilenkov and Valuev [11], Dharma-Wardana and Perrot [12and Lee and More [13]. The best fits are to the recent theory of Redmer [6].

The conductivity versus density curves for all the metals tested have similar appearance, but are shifted along the density axis owing to the different atomic masses. In Fig 8, we present the data contained in Figs. 3-7 on a single plot of conductivity versus atom density rather than mass density. The data appear to cluster around common curves at each temperature, within the experimental fluctuations. It appears therefore that the ion mass has little influence on the conductivity in the density range below solid density. In this figure, we have also compared our data at 10,000K with the tungsten data of Kloss et al. [14] (three large X's), which show close agreement. We also show at 10,000K a point (large solid square) slightly extrapolated from the reflectivity measurements on aluminum of Mostovych and Chan [15].

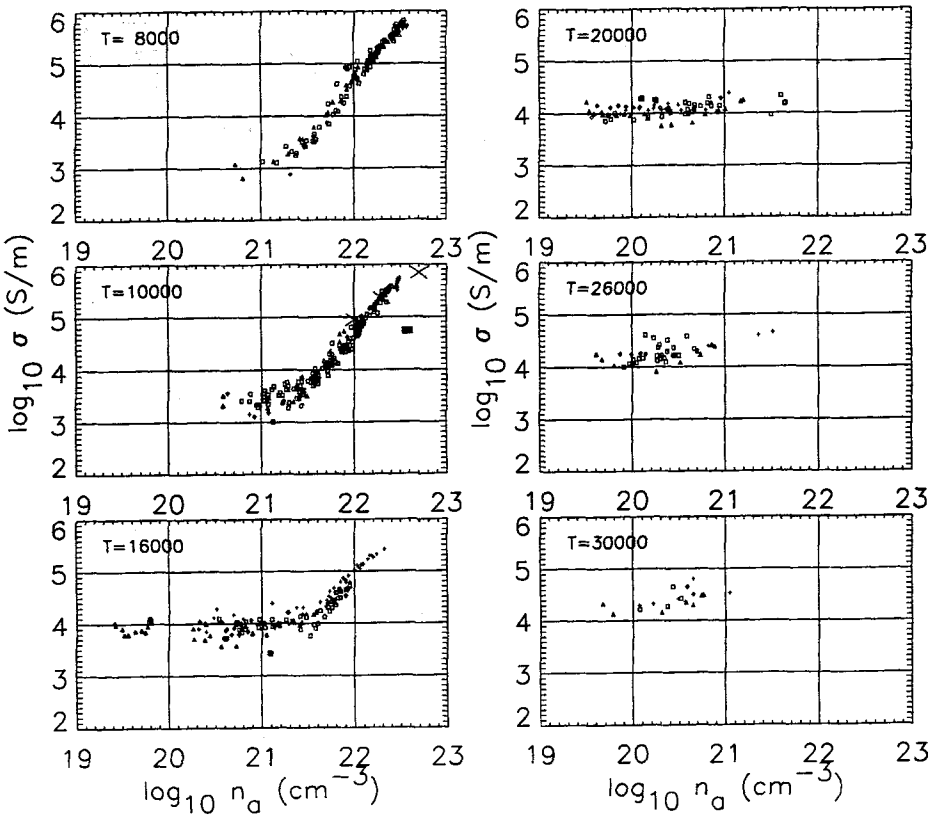

Figure 8. Electrical conductivity versus atom density for the five metals shown in Figs 3-7. □ : aluminum, Δ : iron, ◊ : nickel, x : copper, + : tungsten. On 10,000K plot, three large X's are tungsten data from Kloss et al. [13], solid square is aluminum data from reflectivity measurements of Mostovych and Chan [14].

Acknowledgments

This work was supported by the National Science Foundation. The work would not have been possible without the expert technical help of our now-retired shop supervisor, Kenneth Diller.

References

1. A. W. DeSilva and H.-J. Kunze, Phys. Rev. E 49, 4448 (1994).
2. A. W. DeSilva and J. D. Katsouros, Phys. Rev. E 57, 5945 (1998).
3. Los Alamos National Laboratory Report LA-UR-92-3407 and references therin (undated).
4. M. N. Plooster, Phys. Fluids 13, 2665 (1970).
5. M. H. Rice and J. M. Walsh, J. Chem. Phys. 26, 824 (1957).
6. R. M. More, Adv. in Atomic and Molec. Phys 21, 305 (19850.
7. L. Spitzer, Jr., *Physics of Fully Ionized Plasmas* (Interscience, New York, 1956) p. 86.
8. R. Redmer, Phys. Rev. E 59, 1073 (1999).
9. W. Ebeling, A Förster, V. E. Fortov, V. K. Gryaznov, A Ya. Polishchuk, *Thermophysical Properties of Hot Dense Plasmas*, (B. G. Teubner Verlags. Stuttgart, 1991) pp. 266-285.
10. S. Ichimaru and S. Tanaka, Phys. Rev. A 32, 1790 (1985).
11. Yu. K. Kurilenkov and A. A. Valuev, Beitr. Plasmaphys. 24, 161 (1984).
12. M. W. C. Dharma-wardana and F. Perrot, Phys. Rev E52, 5352 (1995).
13. Y. T. Lee and R. M. More, Phys. Fluids 27:1273 (1984).
14. A. Kloss, T. Motzke, R. Grossjohann, and H. Hess, Phys. Rev. E 54, 5851 (1996).
15. A. N. Mostovych and Y. Chan, Phys. Rev. Lett. 79, 5094 (1997).